Acta Crystallographica Section F
Structural Biology and Crystallization Communications
ISSN 1744-3091

Structure of calcium-bound human S100A13 at pH 7.5 at 1.8 Å resolution

Fabiana Lica Imai,[a] Koji Nagata,[b] Naoto Yonezawa,[a] Minoru Nakano[a]* and Masaru Tanokura[b]

[a]Department of Chemistry, Graduate School of Science, Chiba University, 1-33 Yayoi-cho, Inage-ku, Chiba 263-8522, Japan, and [b]Graduate School of Agricultural and Life Sciences, The University of Tokyo, 1-1-1 Yayoi, Bunkyo-ku, Tokyo 113-8657, Japan

Correspondence e-mail: mnakano@faculty.chiba-u.jp

Received 22 July 2007
Accepted 22 December 2007

PDB Reference: calcium-bound human S100A13, 2egd, r2egdsf.

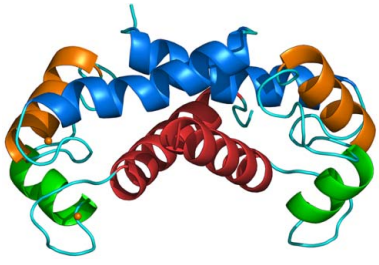

S100A13 is a member of the S100 family of EF-hand-containing calcium-binding proteins. S100A13 plays an important role in the secretion of fibroblast growth factor-1 and interleukin 1α, two pro-angiogenic factors released by the nonclassical endoplasmic reticulum/Golgi-independent secretory pathway. The X-ray crystal structure of human S100A13 at pH 7.5 was determined at 1.8 Å resolution. The structure was solved by molecular replacement and was refined to a final *R* factor of 19.0%. The structure revealed that human S100A13 exists as a homodimer with two calcium ions bound to each protomer. The protomer is composed of four α-helices (α_1–α_4), which form a pair of EF-hand motifs. Dimerization occurs by hydrophobic interactions between helices α_1 and α_4 and by intermolecular hydrogen bonds between residues from helix α_1 and the residues between α_2 and α_3 of both chains. Despite the high similarity of the backbone conformation in each protomer, the crystal structures of human S100A13 at pH 7.5 (this study) and at pH 6.0 [Li *et al.* (2007), *Biochem. Biophys. Res. Commun.* **356**, 616–621] exhibit recognizable differences in the relative orientation (~2.5°) of the protomers within the dimer and also remarkable differences in the side-chain conformations of several amino-acid residues.

1. Introduction

S100-family proteins are small acidic calcium-binding proteins containing two EF-hand motifs: a canonical EF-hand at the C-terminus and an S100-specific EF-hand at the N-terminus. They are expressed in a cell- and tissue-specific manner and have been implicated in intracellular and extracellular regulatory activities (Donato, 1999). Most S100 members exist as homodimers or heterodimers. S100A13 is one of the most recently identified members of the S100 family. Human S100A13 consists of 98 amino-acid residues and has a molecular weight of 11 kDa. Unlike most members of this family, S100A13 is ubiquitously expressed in various tissues (Wicki *et al.*, 1996) and does not expose hydrophobic patches upon Ca^{2+} binding, which is thought to be essential for the interaction of the other S100 proteins with their target proteins (Ridinger *et al.*, 2000).

S100A13 participates in the stress-induced release of the pro-angiogenic polypeptides fibroblast growth factor-1 (FGF-1) and interleukin 1α (IL-1α), which are secreted by the nonclassical endoplasmic reticulum/Golgi-independent pathway (Carreira *et al.*, 1998; Mandinova *et al.*, 2003; Prudovsky *et al.*, 2003). The crystal structures of FGF-1 and IL-1α demonstrated remarkable structural similarity, despite the absence of sequence similarity (Thomas *et al.*, 1985; Zhang *et al.*, 1991). Both Ca^{2+} and Cu^{2+} ions are needed for the interaction of S100A13 with these proteins (Landriscina *et al.*, 2001). The binding of Ca^{2+} to S100A13, which is triggered by Ca^{2+} influx through N-type Ca^{2+} channels (Matsunaga & Ueda, 2006), is likely to form the Cu^{2+}-binding sites on S100A13 (Arnesano *et al.*, 2005). The solution structures of human S100A13 at pH 5.6 in the presence and absence of Ca^{2+} (PDB codes 1yut and 1yur, respectively) have been reported (Arnesano *et al.*, 2005). In addition, the 2.0 Å crystal structure of human S100A13 at pH 6.0 in the presence of Ca^{2+} has very recently been reported (Li *et al.*, 2007). Here, we report the 1.8 Å crystal structure of the Ca^{2+}-bound form of homodimeric human S100A13 at the physiological pH 7.5 and compare it with the solution structures at pH 5.6 and the crystal structure at pH 6.0.

2. Materials and methods

2.1. Expression and purification

Human S100A13 cDNA (GenBank accession No. AK097132) cloned from a first-strand cDNA library from human spleen (Origene Technologies) was amplified by polymerase chain reaction (PCR) and subcloned into the *Nde*I/*Bam*HI site of pET-16b vector (Novagen). *Escherichia coli* BL21(DE3) cells harbouring the expression vector pET-16b-human S100A13 were grown at 310 K. The expression of S100A13 with an N-terminal 10×His tag was induced at an OD_{600} of 0.6 with 1 m*M* isopropyl β-D-1-thiogalactopyranoside (IPTG) and the culture was continued at 310 K for 4 h. The cells were harvested by centrifugation at 3000*g* for 10 min at 277 K, disrupted by sonication and centrifuged at 26 000*g* for 20 min at 277 K. The supernatant was applied onto a His-Bind affinity chromatography column precharged with Ni^{2+} (Novagen). The 10×His-tagged human S100A13 eluted from the resin was digested with factor Xa protease (Novagen, 10 U enzyme per milligram of protein substrate) at room temperature for 4 h, which resulted in human S100A13 with one additional histidine residue at the N-terminus. The cleaved protein was subjected to an Econo-Pac High Q (Bio-Rad) anion-exchange column equilibrated with 25 m*M* Tris–HCl pH 8.1 and eluted with a linear gradient of 0–0.1 *M* NaCl. Fractions containing the purified S100A13 were concentrated to 7.4 mg ml^{-1}.

2.2. Crystallization and data collection

Crystallization experiments were performed using the hanging-drop vapour-diffusion method. Calcium chloride was added to the protein solution to a final concentration of 2 m*M* prior to crystallization in order to obtain the calcium-bound form of S100A13. Crystals were obtained in two weeks by mixing 0.5 µl protein solution

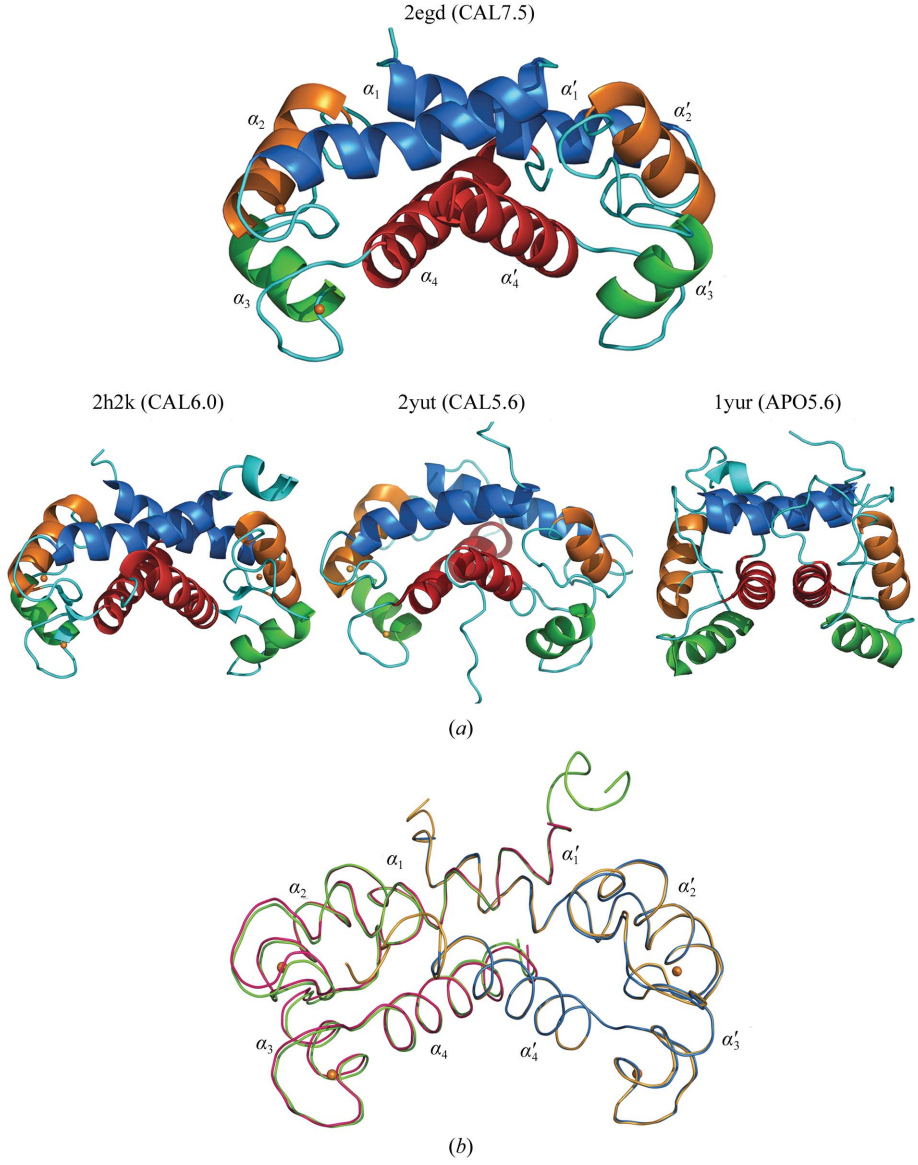

Figure 1
Three-dimensional structures of human S100A13. (*a*) Ribbon diagrams showing the crystal structures of a Ca^{2+}-bound S100A13 homodimer at pH 7.5 (CAL7.5; PDB code 2egd) and at pH 6.0 (CAL6.0; PDB code 2h2k) and the solution structures of Ca^{2+}-bound and Ca^{2+}-free S100A13 at pH 5.6 (CAL5.6 and APO5.6; PDB codes 1yut and 1yur, respectively). The helices in chain *A* are labelled α_1, α_2, α_3, α_4 and the helices in chain *B* are labelled α_1', α_2', α_3', α_4'. Ca^{2+} ions are shown as orange spheres. (*b*) Comparison between the CAL7.5 and CAL6.0 backbone structures. When the *B* chains of CAL7.5 (blue) and CAL6.0 (yellow) are superposed, the *A* chains (pink and green lines for CAL7.5 and CAL6.0, respectively) are placed in slightly different orientations.

Table 1
Summary of data-collection and refinement statistics.

Data-collection statistics	
Wavelength (Å)	1.000
Space group	$P2_12_12_1$
Unit-cell parameters (Å)	a = 39.8, b = 59.3, c = 77.6
Resolution range (Å)	50.0–1.80 (1.86–1.80)
Observed reflections	122381
Unique reflections	17786
Data completeness (%)	99.1 (93.0)
Redundancy	6.9 (6.3)
$R_{\rm merge}$†	0.066 (0.335)
$\langle I/\sigma(I)\rangle$	30.7 (3.4)
Refinement statistics	
Resolution range (Å)	50.0–1.80
R factor (%)	19.0
$R_{\rm free}$ (5.0% total data) (%)	22.7
No. of reflections used for refinement	16686
No. of protein residues	86 (chain A) and 90 (chain B)
No. of Ca^{2+} ions	4
No. of water molecules	101
Average B values (Å^2)	
Protein atoms	25.4
Ca^{2+} ions	23.1
Water O atoms	38.5
R.m.s. bond-length deviations (Å)	0.017
R.m.s. bond-angle deviations (°)	1.378
Ramachandran plot	
Most favoured regions (%)	93.3
Additional allowed regions (%)	6.7
Generously allowed regions (%)	0
Disallowed regions (%)	0

† $R_{\rm merge} = \sum_{hkl}\sum_i |I_i(hkl) - \overline{I(hkl)}|/\sum_{hkl}\sum_i I_i(hkl)$, where $I_i(hkl)$ is the ith observation of reflection hkl and $\overline{I(hkl)}$ is the weighted average intensity for all observations i of reflection hkl.

Table 2
C^α r.m.s. differences between S100A13 structures at pH 7.5 (CAL7.5) and at other pH values.

The residue range used for superposition was 6–90.

(*a*) R.m.s.d. between S100A13 homodimers.

	CAL7.5 (2egd)
CAL7.5 (2egd)	—
CAL6.0 (2h2k)	0.312†/0.326‡
CAL5.6 (1yut)	2.618†/2.610‡
APO5.6 (1yur)	5.952†/5.955‡

(*b*) R.m.s.d. between S100A13 protomers.

	CAL7.5 (2egd)	
	Chain *A*	Chain *B*
CAL7.5 (2egd)		
Chain *A*	—	0.200
Chain *B*	0.222	—
CAL6.0 (2h2k)		
Chain *A*	0.259	0.299
Chain *B*	0.234	0.254
CAL5.6 (1yut)		
Chain *A*	1.909	1.935
Chain *B*	1.998	2.045
APO5.6 (1yur)		
Chain *A*	5.078	5.086
Chain *B*	5.040	5.045

† R.m.s.d. when chains *A* and *B* of CAL7.5 are superposed onto chains *A* and *B*, respectively, of the other S100A13 structure. ‡ R.m.s.d. when chains *A* and *B* of CAL7.5 are superposed onto chains *B* and *A*, respectively, of the other S100A13 structure.

(7.4 mg ml^{-1} in 25 m*M* Tris–HCl pH 8.1, 0.1 *M* NaCl and 2 m*M* $CaCl_2$) and 0.5 µl of a reservoir solution consisting of 22%(*w*/*v*) PEG 3350, 0.1 *M* HEPES–NaOH pH 7.5, 0.2 *M* NaCl and 1.5%(*w*/*v*) 1,2,3-heptanetriol. The drop was equilibrated against 500 µl reservoir solution at 293 K.

X-ray diffraction data were collected on beamline BL41XU at SPring-8 (Harima, Japan). The wavelength was set to 1.000 Å and the distance between the crystal and the detector was set to 200 mm. The diffraction data were indexed, integrated and scaled using *HKL*-2000 (Otwinowski & Minor, 1997). The best crystal diffracted X-rays beyond 1.8 Å resolution and the diffraction data set was scaled to 1.80 Å resolution. The crystal belonged to space group $P2_12_12_1$, with unit-cell parameters a = 39.8, b = 59.3, c = 77.6 Å. The crystal contains two S100A13 molecules in the asymmetric unit ($V_{\rm M}$ = 2.0 Å^3 Da^{-1}, solvent content = 38%).

2.3. Structure determination and refinement

The structure of S100A13 was solved using the *CCP*4 program suite (Collaborative Computational Project, Number 4, 1994). Molecular replacement with *MOLREP* (Vagin & Teplyakov, 1997) produced a good solution when the protein atomic coordinates of S100A8 in the S100A8–S100A9 heterodimer (PDB code 1xk4; I. P. Korndoerfer, F. Brueckner & A. Skerra, unpublished results) were used as the search model. Initial model building was performed with *ARP*/*wARP* (Perrakis *et al.*, 1999). Iterative model fitting and restrained refinement were performed with *Coot* (Emsley & Cowtan, 2004) and *REFMAC*5 (Murshudov *et al.*, 1997). The two S100A13 molecules in the asymmetric unit (chains *A* and *B*) formed a homodimer. TLS (Winn *et al.*, 2001) and restrained refinement in *REFMAC*5 was used as the final refinement, in which the chains *A* and *B* were divided into 14 and 15 TLS groups, respectively. The refined structure was validated with *PROCHECK* (Laskowski *et al.*, 1993). The refined 1.80 Å structure has an *R* factor of 19.0% and a free *R* of 22.7%. The data-collection and refinement statistics are shown in Table 1. Molecular graphics were generated with *PyMOL* (DeLano, 2002). Dimer-interface interactions were analyzed with *PISA* (Krissinel & Henrick, 2005). Interhelical angles were calculated with *MOLMOL* (Koradi *et al.*, 1996). Superpositions of three-dimensional protein structures were made with *CCP*4. The atomic coordinates and experimental structure factors of human S100A13 at pH 7.5 have been deposited in the PDB under code 2egd, where chains *A* and *B* correspond to chains *A* and *B* of PDB entry 2h2k, the crystal structure of human S100A13 at pH 6.0 with the same space group $P2_12_12_1$ and similar unit-cell parameters a = 40.2, b = 60.7, c = 78.5 Å (Li *et al.*, 2007).

3. Results and discussion

The crystallization and preliminary X-ray analysis of S100A13 have previously been reported (Imai *et al.*, 2006). The 1.8 Å crystal structure of human S100A13 at pH 7.5 (referred to in this paper as CAL7.5; PDB code 2egd) was solved by molecular replacement (Fig. 1*a*). S100A13 exists as a homodimer (chains *A* and *B*) with two Ca^{2+} ions bound to each protomer. Each protomer is composed of four α-helices (α_1–α_4), which form a pair of EF-hand motifs. The N-terminal EF-hand (EF1) is composed of helix α_1 (Glu8–Ala24), a Ca^{2+}-binding loop (Arg25–Ser34) and helix α_2 (Val35–Gln45). The C-terminal EF-hand (EF2) is composed of helix α_3 (Leu56–Leu63), a second Ca^{2+}-binding loop (Asp64–Tyr72) and helix α_4 (Phe73–Tyr90). These EF-hands are joined by a hinge region (Leu46–Ser55).

To date, three structures of human S100A13 have been reported: solution structures at pH 5.6 of the Ca^{2+}-bound form (CAL5.6; PDB code 1yut) and of the apo form (APO5.6; PDB code 1yur) (Arnesano *et al.*, 2005) and the 2.0 Å crystal structure at pH 6.0 (CAL6.0; PDB

code 2h2k; Li *et al.*, 2007; Fig. 1*a*). The atomic (C^{α}) r.m.s. differences between our crystal structure (CAL7.5) and these structures at different pH values are shown in Table 2. Comparison with the solution structures shows that CAL7.5 is moderately similar to CAL5.6, while it shows less similarity to APO5.6 because of the conformational changes that occur upon Ca^{2+} binding (Fig. 2*a*). The two crystal structures CAL7.5 and CAL6.0 were both obtained from $P2_12_12_1$ crystals grown by the hanging-drop vapour-diffusion method and had similar unit-cell parameters. The CAL7.5 crystal ($P2_12_12_1$; a = 39.8, b = 59.3, c = 77.6 Å) was obtained from nontagged human S100A13 at pH 7.5 and 293 K with 22%(*w*/*v*) PEG 3350 as the precipitant in the presence of 2 m*M* Ca^{2+}, whereas the CAL6.0 crystal ($P2_12_12_1$; a = 40.2, b = 60.7, c = 78.5 Å) was obtained from human S100A13 with an N-terminal 6×His tag at pH 6.0 and 277 K with 25%(*v*/*v*) PEG MME 550 as the precipitant in the presence of 10 m*M* Ca^{2+}. Chains *A* and *B* of CAL7.5 correspond to chains *A* and *B* of CAL6.0, respectively. CAL7.5 and CAL6.0 are quite similar, with atomic (C^{α}) r.m.s. differences of 0.25 and 0.26 Å for chains *A* and *B*, respectively, and of 0.31 Å overall (Table 2). However, there are recognizable differences between CAL7.5 and CAL6.0 (∼2.5°) in the relative orientations of the protomers within the dimer; when the *B* chains of CAL7.5 and CAL6.0 are superposed, the helices in their *A* chains are differently oriented by 2.2° (α_2), 2.7° (α_3) and 2.6° (α_4) (Fig. 1*b*). Consistently, relatively large r.m.s. differences are seen in helices α_2, α_3 and α_4 as well as in the Ca^{2+}-binding loops (Figs. 1*b* and 2). In addition, side-chain conformational differences are observed for Arg25, Leu41, Ser62, Asn66, Lys72, Asn74, Lys85 and Arg88 in the *A* chains of CAL7.5 and CAL6.0 and for Arg25, Gln26, Glu40, Thr43, Pro47, His48 and Glu82 in the *B* chains of CAL7.5 and CAL6.0 (Fig. 3). With the exception of that of Leu41, all of these side chains are exposed to solvent, indicating that the exposed side chains underwent conformational adjustments when incorporated into the $P2_12_12_1$ crystals at different pH values. On the other hand, the side chain of Leu41 is buried in the molecule and is involved in the hydrophobic cluster. The side-chain conformations of the Leu41 residues in chains *A* and *B* of CAL7.5 and in chain *B* of CAL6.0 are almost the same (χ_2 = 149.2 ± 3.9°), whereas that in chain *A* of CAL6.0 differs (χ_2 = 87.1°). Since the side chains of the four Leu41 residues fit well to the respective $2F_o - F_c$ electron densities with no recognizable $F_o - F_c$ densities (Fig. 3), the side chain of Leu41 of S100A13 can adopt two conformations at pH 6.0. Since most human cells maintain the cytosolic pH at about 7.2 (Alberts *et al.*, 2002), our crystal structure at pH 7.5 (CAL7.5) should reflect the physiologically active form of S100A13.

In the S100-specific EF-hand (EF1) the main-chain carbonyl O atoms of Ala24, Glu27, Arg29 and Ser32, the side-chain O atoms of Glu37 and a water O atom coordinate to a Ca^{2+} ion (Fig. 4*a*), while in the canonical EF-hand (EF2) the main-chain carbonyl O atom of Glu70, the side-chain O atoms of Asp64, Asn66, Asp68 and Glu75, and a water O atom coordinate to a Ca^{2+} ion (Fig. 4*b*). A water molecule of EF1 might interact with the side chain of Glu70 in EF2, forming a possible site of cooperativity of the two EF-hands, as observed by Li *et al.* (2007). The presence of Arg29 in the *Z* position in EF1 of S100A13 is unusual among the Ca^{2+}-binding loops of EF-hand proteins (Marsden *et al.*, 1990). S100A13 differs in Ca^{2+}-binding affinity from other S100 proteins. In general, the four Ca^{2+}-binding sites of homodimeric S100 proteins, *e.g.* S100A2, S100A3, S100A4, S100A5, S100A6 and S100A11, display almost equal affinities for Ca^{2+} ions and a positive cooperativity (Heizmann & Cox, 1998). In contrast, those in S100A13 display two different sets of affinities for Ca^{2+} ions (Ridinger *et al.*, 2000), which indicates that the unusual Arg in the *Z* position of EF1 in S100A13 probably diminishes the Ca^{2+}-binding affinity.

The dimer interface of S100A13 has an accessible surface area of 1380 $Å^2$, covering approximately 24% of the total accessible surface area of each protomer. The interface residues are located in helices α_1 and α_4 and in the hinge region between α_2 and α_3. The dimer interface is mainly built up by hydrophobic interactions between α_1 and α_1', α_4

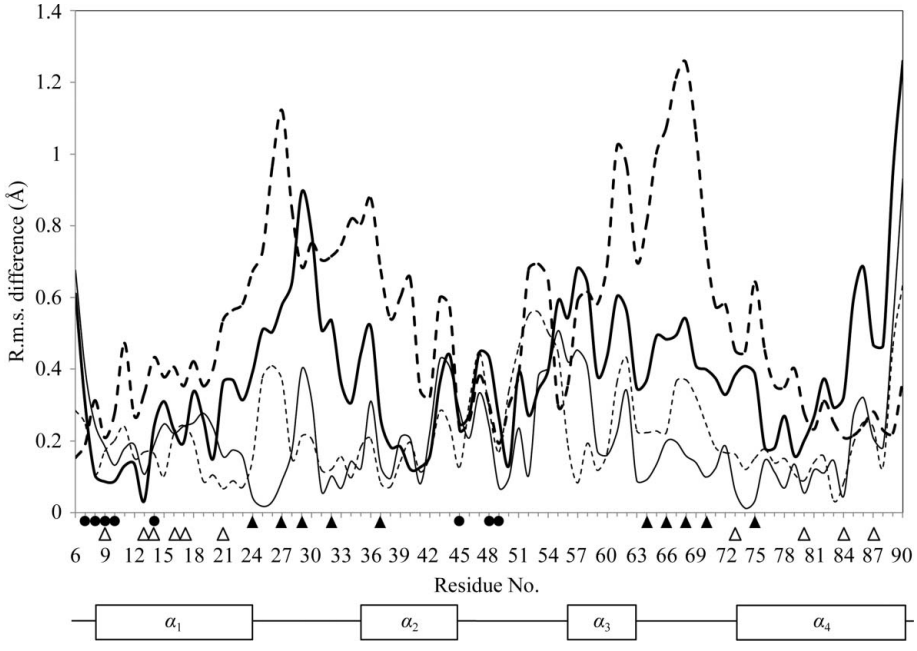

Figure 2
Atomic (C^{α}) r.m.s. difference of each residue between CAL7.5 and CAL6.0. The r.m.s. differences between the *A* chains are shown as thin lines and those between the *B* chains are shown as thin dashed lines when the corresponding chains are superposed. The r.m.s. differences between the *A* chains are shown as thick lines and those between the *B* chains are shown as thick dashed lines when the other chains are superposed. Residues that participate in interchain hydrogen bonds and hydrophobic interactions are indicated by spheres and white triangles, respectively. Ca^{2+}-binding residues are indicated by black triangles. Secondary-structure elements are shown below the graph.

and α_4', α_1 and α_4', and α_4 and α_1' (Figs. 5*a*, 5*b* and 5*c*). The intermolecular hydrogen bonds are mainly located between α_1 and the hinge region of the other protomer, as shown in Fig. 5(*d*). The pattern of intermolecular interactions is similar to those found in the S100A6 homodimer (PDB code 1k9k; Otterbein *et al.*, 2002) and the S100A8/–S100A9 heterodimer (PDB code 1xk4). The dimer-interface residues located in helix α_1 and the hinge region between α_2 and α_3 are well conserved among these S100-family proteins.

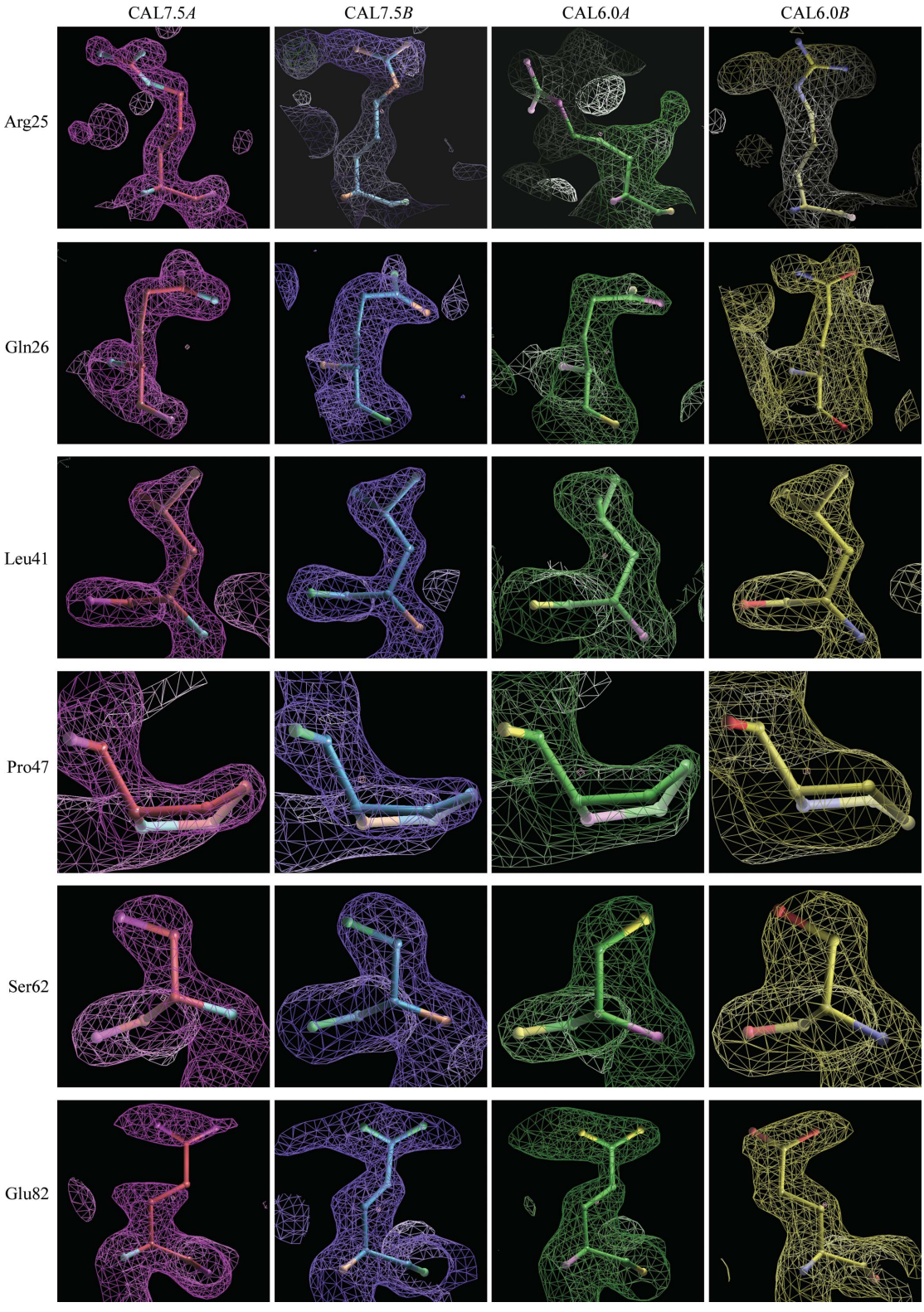

Figure 3
Amino-acid residues with different side-chain conformations in CAL7.5 and CAL6.0. The amino-acid residues and their electron densities were coloured pink, blue, green and yellow for CAL7.5 chain *A*, CAL7.5 chain *B*, CAL6.0 chain *A* and CAL6.0 chain *B*, respectively.

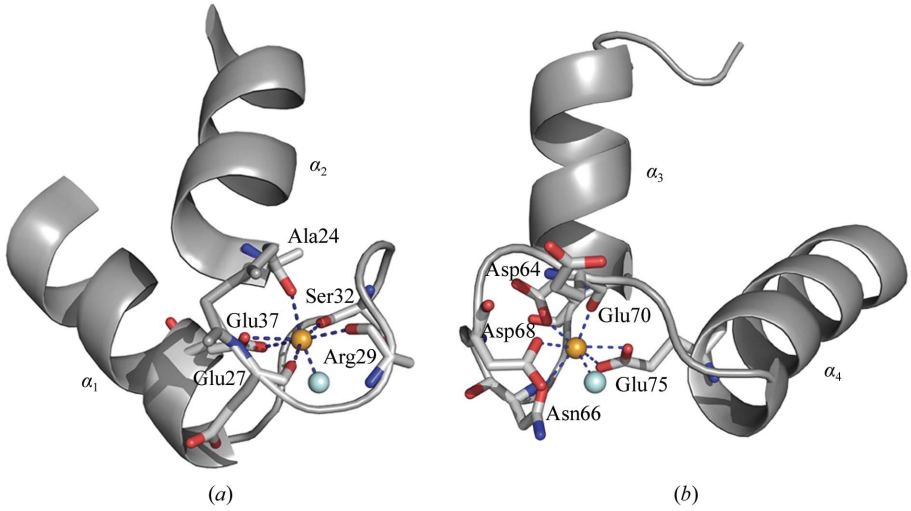

Figure 4
The Ca^{2+}-binding sites of S100A13 in the N-terminal (*a*) and the C-terminal (*b*) EF-hands. The residues that participate in the coordination of Ca^{2+} are shown as stick models. The bound Ca^{2+} ion is shown as an orange sphere and the coordinating water molecule is shown as a cyan sphere.

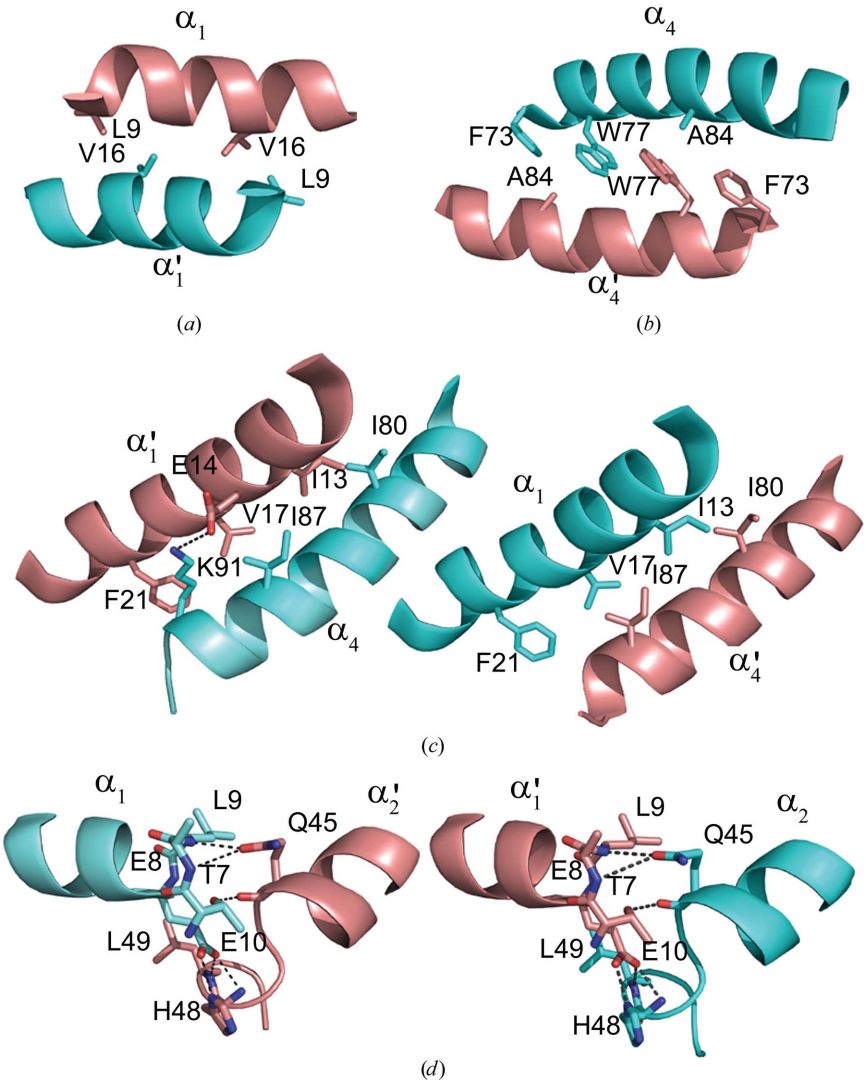

Figure 5
The dimer interface of the S100A13 homodimer. The segments of chains *A* and *B* are coloured pink and cyan, respectively. (*a*) The interface between helices α_1 and α_1'. (*b*) The interface between α_4 and α_4'. (*c*) The interface between α_1/α_4' and α_1'/α_4. (*d*) Intermolecular hydrogen bonds between α_1 and the hinge region. Thr7 ($O^{\gamma 1}$), Glu8 (N), Leu9 (N), Glu10 ($O^{\varepsilon 1}$ and $O^{\varepsilon 2}$), Gln45 (O and $O^{\varepsilon 1}$), His48 (N and $N^{\delta 1}$) and Leu49 (N) of both chains participate in the hydrogen bonding between the protomers. The side chains involved in the dimer interface are shown in the stick model. O and N atoms are coloured red and blue, respectively. Hydrogen bonds are shown as broken lines.

S100A13 can form a multiprotein complex with FGF-1 and p40 synaptotagmin (Carreira *et al.*, 1998; Landriscina *et al.*, 2001). This ternary complex formation is essential for the stress-induced release of FGF-1, which is inhibited by the anti-inflammatory drug amlexanox (Carreira *et al.*, 1998), a specific binder of S100A13 (Shishibori *et al.*, 1999). FGF-1 is a pro-angiogenic factor that induces endothelial cell proliferation and differentiation and plays an important role in chronic inflammatory diseases (Lai & Adams, 2005) such as rheumatoid arthritis (Malemud, 2007). A VAST structural-homology search (http://www.ncbi.nlm.nih.gov/structure/VAST/vastsearch.html) revealed the structural similarity of the S100A13 homodimer (CAL7.5) to the S100A8–S100A9 heterodimer (PDB code 1xk4) and the S100A1 homodimer (PDB code 1zfs; Wright *et al.*, 2005), with r.m.s. differences of 1.2 and 2.5 Å, respectively. Interestingly, these structurally similar proteins are functionally related to inflammatory conditions. The S100A1 homodimer binds amlexanox (Okada *et al.*, 2002) as does S100A13, while the S100A8–S100A9 heterodimer, which is implicated in Ca^{2+}-dependent functions during inflammation (Odink *et al.*, 1987), is expressed in human peripheral blood mononuclear cells under inflammatory conditions and in rheumatoid arthritis (Brun *et al.*, 1992).

The basic C-terminal part of S100A13 has a flexible character as in S100A9 (Itou *et al.*, 2002) as shown by the unobserved electron densities for the C-terminal eight and three residues (91–98 and 96–98) in chains *A* and *B* of CAL7.5, respectively. The C-terminus of chain *B* is less flexible owing to the crystal packing. Since the C-terminal region is implicated in intermolecular interaction with FGF-1 and amlexanox, the flexible character of this region would be important for the ternary complex formation for FGF-1 secretion (Landriscina *et al.*, 2001).

Synchrotron-radiation experiments were performed at SPring-8 (Harima, Japan) with the approval of the Japan Synchrotron Radiation Research Institute (Proposal Nos. 2006A2721 and 2006A2728). This work was supported in part by the National Project on Protein Structural and Functional Analyses (NPPSFA) and Targeted Proteins Research Program (TPRP) of the Ministry of Education, Culture, Sports, Science and Technology of Japan and by the Grants-in-Aid from The Japan Society for the Promotion of Science (JSPS).

References

Alberts, B., Johnson, A., Lewis, J., Raff, M., Roberts, K. & Walter, P. (2002). *Molecular Biology of the Cell*, p. 622. New York/London: Garland Science.
Arnesano, F., Banci, L., Bertini, I., Fantoni, A., Tenori, L. & Viezzoli, M. S. (2005). *Angew. Chem. Int. Ed.* **44**, 2–5.
Brun, J. G., Haga, H. J., Boe, E., Kallay, I., Lekven, C., Berntzen, H. B. & Fagerhol, M. K. (1992). *J. Rheumatol.* **19**, 859–862.
Carreira, C. M., La Vallee, T. M., Tarantini, F., Jackson, A., Lathrop, J. T., Hampton, B., Burgess, W. H. & Maciag, T. (1998). *J. Biol. Chem.* **273**, 22224–22231.
Collaborative Computational Project, Number 4 (1994). *Acta Cryst.* D**50**, 760–763.
DeLano, W. L. (2002). *The PyMOL Molecular Graphics System.* http://www.pymol.org/.
Donato, R. (1999). *Biochim. Biophys. Acta*, **1450**, 191–231.
Emsley, P. & Cowtan, K. (2004). *Acta Cryst.* D**60**, 2126–2132.
Heizmann, C. W. & Cox, J. A. (1998). *Biometals*, **11**, 383–397.
Imai, F. L., Nagata, K., Yonezawa, N., Yu, J., Ito, E., Kanai, S., Tanokura, M. & Nakano, M. (2006). *Acta Cryst.* F**62**, 1144–1146.
Itou, H., Yao, M., Fujita, I., Watanabe, N., Suzuki, M., Nishihira, J. & Tanaka, I. (2002). *J. Mol. Biol.* **316**, 265–276.
Koradi, R., Billeter, M. & Wüthrich, K. (1996). *J. Mol. Graph.* **14**, 51–55.
Krissinel, E. & Henrick, K. (2005). *CommpLife 2005*, edited by M. R. Berthold, R. Glen, K. Diederichs, O. Kohlbacher & I. Fischer, pp. 163–174. Berlin/Heidelberg: Springer-Verlag.
Lai, W. K. & Adams, D. H. (2005). *J. Hepatol.* **42**, 7–11.
Landriscina, M., Bagala, C., Mandinova, A., Soldi, R., Micucci, I., Bellum, S., Prudovsky, I. & Maciag, T. (2001). *J. Biol. Chem.* **276**, 25549–25557.
Laskowski, R. A., MacArthur, M. W., Moss, D. S. & Thornton, J. M. (1993). *J. Appl. Cryst.* **26**, 283–291.
Li, M., Zhang, P. F., Pan, X. W. & Chang, W. R. (2007). *Biochem. Biophys. Res. Commun.* **356**, 616–621.
Malemud, C. J. (2007). *Clin. Chim. Acta*, **375**, 10–19.
Mandinova, A., Soldi, R., Graziani, I., Bagala, C., Bellum, S., Landriscina, M., Tarantini, F., Prudovsky, I. & Maciag, T. (2003). *J. Cell Sci.* **116**, 2687–2696.
Marsden, B. J., Shaw, G. S. & Sykes, B. D. (1990). *Biochem. Cell Biol.* **68**, 587–601.
Matsunaga, H. & Ueda, H. (2006). *Cell. Mol. Neurobiol.* **26**, 237–246.
Murshudov, G. N., Vagin, A. A. & Dodson, E. J. (1997). *Acta Cryst.* D**53**, 240–255.
Odink, K., Cerletti, N., Bruggen, J., Clerc, R. G., Tarcsay, L., Zwadlo, G., Gerhards, G., Schelegel, R. & Sorg, C. (1987). *Nature (London)*, **330**, 80–82.
Okada, M., Tokumitsu, H., Kubota, Y. & Kobayashi, R. (2002). *Biochem. Biophys. Res. Commun.* **292**, 1023–1030.
Otterbein, L. R., Kordowska, J., Witte-Hoffmann, C., Wang, C.-L. A. & Dominguez, R. (2002). *Structure*, **10**, 557–567.
Otwinowski, Z. & Minor, W. (1997). *Methods Enzymol.* **276**, 307–326.
Perrakis, A., Morris, R. & Lamzin, V. S. (1999). *Nature Struct. Biol.* **6**, 458–463.
Prudovsky, I., Mandinova, A., Soldi, R., Bagala, C., Graziani, I., Landriscina, M., Tarantini, F., Duarte, M., Bellum, S., Doherty, H. & Maciag, T. (2003). *J. Cell Sci.* **116**, 4871–4881.
Ridinger, K., Schafer, B. W., Durussel, I., Cox, J. A. & Heizmann, C. W. (2000). *J. Biol. Chem.* **275**, 8686–8694.
Shishibori, T., Oyama, Y., Matsushita, O., Yamashita, K., Furuichi, H., Okabe, A., Maeta, H., Hata, Y. & Kobayashi, R. (1999). *Biochem. J.* **338**, 583–589.
Thomas, K. A., Rios-Candelore, M., Gimenez-Gallego, G., DiSalvo, J., Bennett, C., Rodkey, J. & Fitzpatrick, S. (1985). *Proc. Natl Acad. Sci. USA*, **82**, 6409–6413.
Vagin, A. & Teplyakov, A. (1997). *J. Appl. Cryst.* **30**, 1022–1025.
Wicki, R., Schafer, B. W., Erne, P. & Heizmann, C. W. (1996). *Biochem. Biophys. Res. Commun.* **227**, 594–599.
Winn, M. D., Isupov, M. N. & Murshudov, G. N. (2001). *Acta Cryst.* D**57**, 122–133.
Wright, N. T., Varney, K. M., Ellis, K. C., Markowitz, J., Gitti, R. K., Zimmer, D. B. & Weber, D. J. (2005). *J. Mol. Biol.* **353**, 410–426.
Zhang, J. D., Cousens, L. S., Barr, P. J. & Sprang, S. R. (1991). *Proc. Natl Acad. Sci. USA*, **88**, 3446–3450.